Struct Multidisc Optim (2015) 51:385–396
DOI 10.1007/s00158-014-1133-8

RESEARCH PAPER

Incorporating fabrication cost into topology optimization of discrete structures and lattices

Alireza Asadpoure · James K. Guest · Lorenzo Valdevit

Received: 17 October 2013 / Revised: 5 May 2014 / Accepted: 23 June 2014 / Published online: 19 August 2014

Abstract In this article, we propose a method to incorporate fabrication cost in the topology optimization of light and stiff truss structures and periodic lattices. The fabrication cost of a design is estimated by assigning a unit cost to each truss element, meant to approximate the cost of element placement and associated connections. A regularized Heaviside step function is utilized to estimate the number of elements existing in the design domain. This makes the cost function smooth and differentiable, thus enabling the application of gradient-based optimization schemes. We demonstrate the proposed method with classic examples in structural engineering and in the design of a material lattice, illustrating the effect of the fabrication unit cost on the optimal topologies. We also show that the proposed method can be efficiently used to impose an upper bound on the allowed number of elements in the optimal design of a truss system. Importantly, compared to traditional approaches in structural topology optimization, the proposed algorithm reduces the computational time and reduces the dependency on the threshold used for element removal.

Keywords Fabrication cost · Material cost · Minimum weight · Topology optimization · Lattices

A. Asadpoure · L. Valdevit (✉)
Mechanical and Aerospace Engineering, University of California Irvine, Irvine, CA 92697, USA
e-mail: valdevit@uci.edu

A. Asadpoure
e-mail: asadpoua@uci.edu

J. K. Guest
Department of Civil Engineering, Johns Hopkins University, Baltimore, MD 21218, USA
e-mail: jkguest@jhu.edu

1 Introduction

Structural topology optimization is a powerful method for the identification of the optimized distributions of material within a design domain. When applied to truss (or frame) structures or periodic lattices, topology optimization seeks the best location and cross-section of each member within the design domain (the external shape of the structure or the unit cell). This can be conveniently implemented with the ground structure method (Dorn et al. 1964), in which a very dense initial mesh is generated and inefficient elements are subsequently removed from the design domain following the optimization. The cross-sectional area of each member can be modeled as a continuous design variable, thus allowing the application of gradient-based schemes.

Although used extensively in literature, a drawback of the ground structure approach is its tendency to produce complex topologies for nontrivial problems optimizing structural stiffness. Such topologies may result from convex problem formulations (Ben-Tal and Bendsøe 1993; Bendsøe et al. 1994), and thus can be proven to be globally optimal for the considered ground structure. A potential means of inhibiting topological complexity is to remove members with cross-sectional area below a threshold set by the designer. The problem can then be solved again using the previous final solution as the initial guess, and material volume that is freed up through the thresholding can be re-assigned to members remaining in the topology. While a practical strategy, global optimality is lost in this process and the chosen threshold magnitude may have dramatic effect on the optimal topology. The threshold may also require multiple increases before a structure with reasonable topological complexity is identified.

Another strategy for preventing complexity is to penalize intermediate values of cross-sectional areas (i.e. cross-sectional areas between the minimum and maximum allowed values) using the continuum-based Solid Isotropic Material with Penalization (SIMP) method (Bendsøe 1989; Zhou and Rozvany 1991). In this approach, the stiffness of an element is artificially modified so that it scales non-linearly with the cross-sectional area (thus remaining very low for all areas far from the maximum value). This method is extremely effective in continuum domains in which the design variables are binary (i.e., local existence or nonexistence of material), and has also been shown to reduce complexity of truss topologies with continuous design variables (Amir and Sigmund 2013). However, when small magnitudes of penalization are used, intermediate cross-sections may still appear in the final solution. Although intermediate cross-sections are quite natural for lattice structures, their stiffness is misrepresented to the optimizer and thus the designed system will actually exhibit suboptimal performance when analyzed under actual (non-penalized) conditions. When large magnitudes of penalization are used, the solution will tend towards all members having the same (maximum) cross-section. In this case, one is essentially determining whether each element is to exist in the final topology or not (e.g., in the design of periodic lattices with beam elements (Sigmund 1995)).

At the heart of the complexity property is that the ground structure approach to maximum stiffness design is generally non-convergent (Rozvany 2011), making solutions highly dependent on the choice of the ground structure. As new elements cannot be added during the optimization process, the ground structure must be complex enough to incorporate a very large number of reasonable designs. Generally speaking, the maximum achievable stiffness (minimum compliance) improves as nodes and elements are added to the ground structure and, typically, topological complexity follows.

From a practical standpoint, structures and lattices that are topological complex may be prohibitively expensive to manufacture. In the absence of a quantitative cost-benefit analysis that compares cost and performance of near-optimal designs of varying complexity, this optimization tool is of limited use to the engineer. To the authors' knowledge, the total cost of lattice structures has only been modeled as a function of the amount of material used, either through an explicit material volume (or mass) objective function or constraint, or through a complexity parameter related to material use. Regarding the latter, Parkes (1975), for example, suggested to penalize the complexity of structures by adding a constant length to each element at each joint (which was called the "joint radius"). The penalization of shorter elements is proportional to their cross-sectional area, and hence is a linear function of material cost.

From a practical perspective, the cost of fabricating a topologically complex lattice or a discrete structure is only partly related to the cost of the material; i.e., two designs with the same mass (and hence amount of material) but different topological complexity will generally have very different fabrication costs. In this paper, we propose a more comprehensive cost function, which combines both the cost of material and the fabrication cost associated with fabricating each structural member within the lattice. As the material cost scales linearly with the mass of the structure, the proposed approach conveniently enables a cost-benefit analysis between mass and design complexity. A regularized Heaviside step function is utilized to account for costs associated with each member, thus enabling the application of gradient-based approaches. We illustrate the advantages of the proposed cost function with two classic examples of maximally stiff and light structures. Finally, to demonstrate the versatility of the suggested function, a minimum deflection problem with an imposed upper bound on the number of elements is investigated.

It is worth pointing out that continuum topology optimization for maximum stiffness faces similar issues of mesh dependency and the optimal results tending towards complex topologies. This has been studied extensively in literature and is typically circumvented through restriction of the design space. Examples include the perimeter constraint on topology boundaries (Ambrosio and Buttazzo 1993; Haber et al. 1996), minimum member length scale constraints (Poulsen 2003), and minimum length scale enforcing projection methods (Guest 2009; Guest et al. 2004) and nonlinear filters (Sigmund 2007). As these restrictions are tightened, design complexity and fabrication cost is reduced. In fact, the regularized Heaviside function used herein is borrowed from the original continuum Heaviside Projection algorithm for enforcing a minimum length scale on structural members (Guest et al. 2004).

Although all the examples in this article refer to continuous cross-section area variables and total cost optimization under stiffness constraints, the proposed method is generally applicable to virtually any mechanical (and multifunctional) constraints (e.g., bounds on yielding or buckling strength), as well as problems where cross-section variables must be selected from discrete set of available sizes (Achtziger and Stolpe 2006, 2007a, b; Groenwold et al. 1996; Stolpe 2004; Zhu et al. 2014). For further details on topology optimization of lattices, including other mechanical objectives and their challenges, readers are referred to Bendsøe and Sigmund (2003) and Rozvany (1996).

2 Minimum cost in structural topology optimization

We consider the common problem in topology optimization of trusses (or frames) of minimizing weight (or material cost) under allowable deflection constraints. As discussed in the introduction, nearly every topology optimization algorithm for discrete domains, such as frame structures, starts with a dense ground structure mesh; as the optimization procedure progresses, inefficient elements are removed from the design domain. Without loss of generality we only consider truss elements, characterized by a single design variable (the cross-sectional area). Extension of the proposed algorithm to beam elements is straightforward. The Finite Element method is employed for calculation of displacements. The weight (or material cost) optimization problem for a discretized domain (Ω) can then be expressed as:

$$\min_{\boldsymbol{\rho}} \quad W(\boldsymbol{\rho}) = \min_{\boldsymbol{\rho}} \sum_{\forall e \in \Omega} \alpha_W^e \gamma^e \rho^e v^e \tag{1}$$

$$s.t. \quad \mathbf{K}(\boldsymbol{\rho})\,\mathbf{d} = \mathbf{f} \tag{2}$$

$$C_i(\boldsymbol{\rho}) \leq C_i^* \quad for\ i = 1..N \tag{3}$$

$$0 \leq \rho^e \leq 1 \quad \forall e \in \Omega \tag{4}$$

Here $\boldsymbol{\rho}$ is the vector of design variables, assembling the non-dimensionalized cross-sectional areas of each element, ρ^e ($\rho^e = A^e/A_{max}$, with A_{max} the maximum allowed cross-sectional area); W is the weight of the lattice in the design domain; γ^e is the weight density of the material used for element e; v^e is a quantity giving the volume of the element e if multiplied by ρ^e (i.e., $v^e = A_{max} L_e$); C_i^* is the maximum allowable deflection constraint i, N is the number of deflection constraints, α_W^e is the material cost per unit weight of element e, and C_i is the deflection constraint i, computed as follows:

$$C_i(\boldsymbol{\rho}) = \mathbf{L}_i^T \mathbf{d}(\boldsymbol{\rho}) \tag{5}$$

where $\mathbf{d}$ is the vector of nodal displacements, obtained by solving the discretized equilibrium equation, $\mathbf{Kd} = \mathbf{f}$ with $\mathbf{K}$ and $\mathbf{f}$ the global stiffness matrix and applied load vector, respectively; finally, $\mathbf{L}_i$ is a vector that extracts the desired displacement (or combines multiple displacements) from $\mathbf{d}$. When constraining the deflection at a single degree of freedom i, the vector $\mathbf{L}_i$ has only one non-zero component corresponding to degree of freedom i. The element stiffness matrix defined in the parent domain is given as

$$\mathbf{k}^e\left(\rho^e\right) = \left((1-\rho_{min})\,\rho^e + \rho_{min}\right) \frac{E A_{max}}{L^e} \begin{bmatrix} 1 & -1 \\ -1 & 1 \end{bmatrix} \tag{6}$$

where E is the Young's modulus of the constituent material, L^e is the element length of element e, and ρ_{min} is a small positive number to maintain positive definiteness of the global stiffness matrix during the optimization process. Once the optimization algorithm solving (1)–(4) converges, an element e remains in the structure only if its design variable ρ^e is greater than a threshold value.

The fabrication cost of the entire domain can be estimated by accounting for the presence of all the remaining elements. The idea is that any element existing in the structure incurs a placement cost and cost for making two connections, one at either end. This model is particularly suitable to the construction of structures, such as bridges, in which installation costs for each element can be readily quantified. Importantly, the same model is also meaningful for Additive Manufacturing (AM) processes. Although the placement cost of an element is not well defined in AM processes, increasing the number of elements in a structure (or lattice unit cell) of a given size will generally reduce their dimension and hence increase the structural hierarchy of the design. This obviously increases the fabrication time, and hence the manufacturing cost. As the number of elements is not a differentiable function, a regularized Heaviside step function is used to ensure that the fabrication cost function be smooth and consequently differentiable, thus maintaining the advantage of using gradient-based optimizers. One can then extend the minimum cost problem stated in (1)–(4) to minimum material and fabrication cost minimization as follows:

$$\min_{\boldsymbol{\rho}} \quad W(\boldsymbol{\rho}) + F(\boldsymbol{\rho}) = \min_{\boldsymbol{\rho}} \sum_{\forall e \in \Omega} \alpha_W^e \gamma^e \rho^e v^e + \sum_{\forall e \in \Omega} \alpha_F^e \,\mathrm{H}\left(\rho^e\right) \tag{7}$$

$$s.t. \quad \mathbf{K}(\boldsymbol{\rho})\,\mathbf{d} = \mathbf{f} \tag{8}$$

$$C_i(\boldsymbol{\rho}) \leq C_i^* \quad for\ i = 1..N \tag{9}$$

$$0 \leq \rho^e \leq 1 \quad \forall e \in \Omega \tag{10}$$

where α_F^e is the fabrication cost associated with element e, $F(\boldsymbol{\rho})$ is total fabrication cost, and H is a regularization of the Heaviside step function, defined as follows (Guest et al. 2004):

$$\mathrm{H}\left(\rho^e\right) = 1 - \exp\left(-\beta\rho^e\right) + \rho^e \exp(-\beta) \tag{11}$$

where β is a shaping parameter for the regularization. As $\beta \rightarrow \infty$, the above function approaches the Heaviside function and any element with $\rho^e > 0$ will count towards the fabrication cost (see Guest et al. (2011) for detailed discussion).

Equation (7) represents a simple smooth function that combines fabrication cost and material cost. In this equation, the value of α_F^e is dependent on the fabrication procedure for element e. In the construction of structures, for example, this parameter for each structural element may include the cost of crane time and labor necessary to position the element, and the labor cost of making two connections. More elaborate functions combining the two costs can be implemented, but this simple function captures the necessary features and has a strong influence on the optimized topology as will be demonstrated in the numerical examples below. It is worth mentioning that the problem formulation in (7)–(10) considers only deflection constraints under linear elasticity, and ignores possible strength constraints (for buckling or yielding) or other design requirements. These can be added as needed, without changing the structure of the model or conclusions. The scope of this work is to investigate how the fabrication cost function influences topology. The reader is referred to Bendsøe and Sigmund (2003) for a review of other such constraints and solution strategies.

An important beneficial byproduct of using this objective function is that the optimizer avoids designing members with very small cross-sections when a sufficiently large fabrication cost is introduced. This makes identifying elements for removal extremely objective circumventing the usual reliance on the arbitrary thresholding parameter. This will be demonstrated quantitatively in the numerical example (Section 3).

Derivatives of (7) with respect to design variable can be computed by:

$$\frac{d}{d\rho^e}\left(W(\boldsymbol{\rho}) + F(\boldsymbol{\rho})\right) = \alpha_W^e \gamma^e v^e + \alpha_F^e \left(\beta \exp\left(-\beta\rho^e\right) + \exp(-\beta)\right) \tag{12}$$

where $d/d\rho^e$ denotes the (full) derivative with respect to ρ^e. Derivatives of (9) can be computed using the adjoint method as:

$$\frac{dC_i}{d\rho^e} = -\boldsymbol{\lambda}_i^T \frac{d\mathbf{K}}{d\rho^e}\mathbf{d} = -\boldsymbol{\lambda}_i^{eT} \frac{d\mathbf{K}^e}{d\rho^e}\mathbf{d}^e \tag{13}$$

where

$$\mathbf{K}\boldsymbol{\lambda}_i = \mathbf{L}_i \tag{14}$$

and the superscript ^{e} for each vector or matrix denotes the elemental level of that vector or matrix for element e.

A conceptually different approach to accounting for fabrication cost is to constrain the maximum allowable number of elements appearing in the optimized design. Practically, this optimization represents a situation where the maximum allowable fabrication cost is well defined or, for example, there is a maximum number of elements that can be installed due to transportation considerations, time to construction, or available connection components. The functions described previously in this section can be equivalently applied to this formulation, to handle a discrete variable (the number of elements) with a gradient-based approach. If the objective is stiffness maximization (i.e., deflection or compliance minimization), this alternative optimization problem can be stated as follows:

$$\min_{\boldsymbol{\rho}} \; C(\boldsymbol{\rho}) = \min_{\boldsymbol{\rho}} \; \mathbf{L}^T \mathbf{d}(\boldsymbol{\rho}) \tag{15}$$

$$s.t. \;\; \mathbf{K}(\boldsymbol{\rho})\,\mathbf{d} = \mathbf{f} \tag{16}$$

$$\sum_{\forall e \in \Omega} \mathrm{H}\left(\rho_x^e\right) \leq n_{el}^* \tag{17}$$

$$0 \leq \rho^e \leq 1 \quad \forall e \in \Omega \tag{18}$$

where n_{el}^* is the maximum allowable number of elements, and all the other variables are defined as before. Derivatives of (15) and (17) can be obtained using (13) and the second term in the parentheses of the right hand side of (12), respectively.

3 Numerical examples

We apply the proposed minimum cost design algorithm (7)–(10) to two classic 2D truss problems and to the design of a periodic lattice. We also provide an example for the optimization problem stated by (15)–(18). For all examples, the Method of Moving Asymptotes (MMA) (Svanberg 1987; 1995) is used to solve the optimization problem. For problems in which the fabrication cost is significant, i.e. more than 5 % of the total cost, we use a modification of MMA proposed by Guest et al. (2011). Using this modification allows avoiding a continuation step on the parameter β in (11), which would otherwise be required to ensure convergence. After convergence, elements with design variable ρ_e below the threshold are removed and the problem is solved again using the converged solution as the initial guess. This is repeated until no element with design variable lower than the threshold is found.

In practice, unit material costs α_W^e and unit fabrication costs α_F^e are dictated by local markets and methods where the structure or lattices are to be fabricated. To clearly illustrate the algorithm, however, all examples herein use a fixed magnitude of $\alpha_W^e = \alpha_W$ and only α_F^e is varied with $\alpha_F^e = \alpha_F$, i.e. uniform weight cost and fabrication cost function for all elements, unless otherwise stated. Without loss of generality, symmetry about a vertical axis passing through the load application point is imposed to reduce the number of design variables. Nonetheless, the whole symmetric structure is modeled, allowing the development of elements crossing the line of symmetry in optimized solutions (e.g., horizontal elements connecting pairs of symmetrical nodes

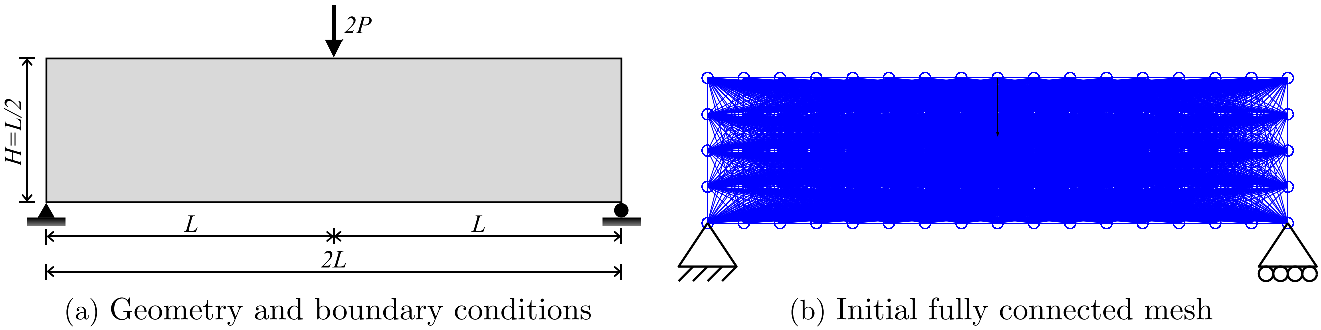

Fig. 1 A simply supported domain with a point load on the top boundary **(a)** geometry and boundary conditions; **(b)** initial fully connected mesh with 17 × 5 nodes and 3,570 truss elements

on two sides of the line of symmetry). In the following examples, initial meshes used for optimization consist of overlapping elements and no specific algorithm, other than the proposed, is used to avoid development of overlapping elements in the final structure.

3.1 A simply supported truss structure with a point load on the top boundary

Figure 1a illustrates the geometry and boundary conditions of a simply supported domain with a point load applied at the middle of the top boundary. The ground structure features a fully connected lattice with 17 × 5 nodes, consisting of 3570 truss elements connecting all the possible pairs of nodes as shown in Fig. 1b. The removal threshold for cross-sectional area of elements is set at $\rho^e_{th} = 10^{-5}$ and a single maximum allowable deflection constraint is applied at midspan with $C^* = 1600P/EL$, where P is the magnitude of the applied load and E the Young's modulus of the material.

The optimization is performed for $\alpha_W = (10/L)^3$ and $\alpha_F = \{0, 10^{-1}, 10^0, 10^1\}$, resulting in a total of 4 independent optimization runs. The optimized solutions for different values of α_F are shown in Fig. 2. As expected, the number of elements in the optimal design is reduced as the fabrication cost of elements increases. This happens at the cost of a heavier structure, i.e. more material is needed to meet the same stiffness constraint (Fig. 3). Both material and fabrication costs are normalized with the corresponding values for the $\alpha_F = 0$ optimized structure in Fig. 2a. Notice that for $\alpha_F \leq 10^{-1}$, the optimal topology (and hence the material and fabrication cost) is constant for the considered ground structure. If α_F is increased to 10^0, the number of elements in the optimal design drops by 70 %, with only a 5 % increase in the material cost (and hence the weight of the structure). A further increase to $\alpha_F = 10^1$ reduces the number of elements to the minimum possible for the problem (3), but this requires a 35 % increase in weight. For any larger α_F, the solution will stay the same. Notice that even for situations where the fabrication cost is not well defined, this study would reveal the optimum compromise between mechanical efficiency and ease of fabrication (in this case, the design in Fig. 2b).

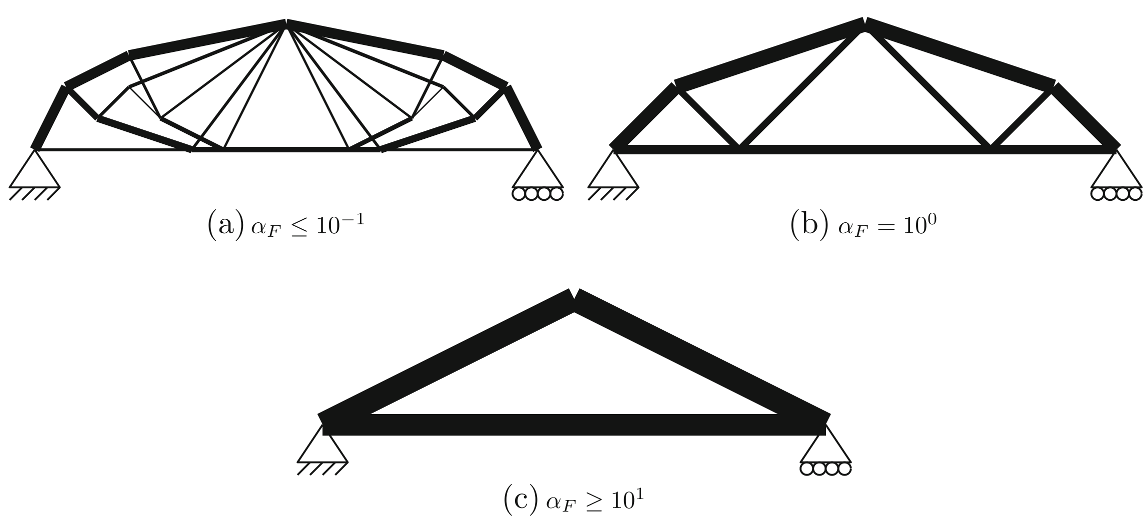

Fig. 2 Optimized truss structures for the simply supported domain shown in Fig. 1 for different values of fabrication unit cost α_F

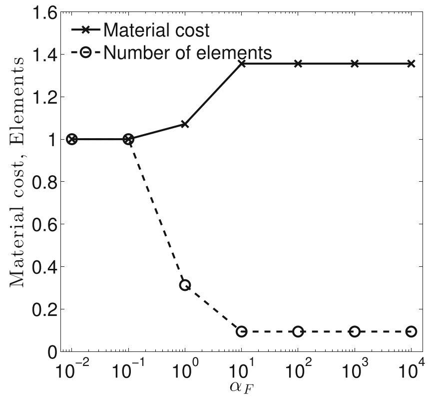

Fig. 3 Material cost and the number of elements in optimized structures for the domain shown in Fig. 1 for different fabrication unit costs of α_F; All values are normalized with the corresponding value for the optimized structure shown in Fig. 2a with zero fabrication cost, i.e. $\alpha_F = 0$

An interesting byproduct of the proposed approach to incorporating fabrication cost is that elements with very small but nonzero cross-sectional areas are naturally driven to zero area by the optimizer, to eliminate their contribution to the fabrication cost. This creates a separation between "structural" and "non-structural" elements, thereby reducing the influence of the arbitrarily selected threshold used in conventional approaches to identify elements that are to be removed from the ground structure. This approach also reduces the number of optimization iterations to convergence, thereby substantially reducing the computational cost. As an example, consider the optimized designs shown in Fig. 2a for $\alpha_F = 0$ and 10^{-1}. The optimized structure for these two values of α_F is identical and therefore both designs have the same amount of material, but the convergence rate for $\alpha_F = 10^{-1}$ is about 20 % higher than for $\alpha_F = 0$. This behavior is quantitatively illustrated in Fig. 4, which shows the distribution of design variables after the first optimization convergence, i.e. before the first round of element removal. Clearly, increasing α_F results in more elements dropping significantly below the threshold and fewer elements around the threshold, resulting in faster convergence.

3.2 A simply supported truss structure with a point load on the bottom boundary (Wheel-like problem)

Geometry and boundary conditions for a simply supported domain with a point load applied at the middle of the bottom boundary are illustrated in Fig. 5a. This design domain is similar to the structural part of the well-known wheel problem (Jog et al. 1994), with the difference that only

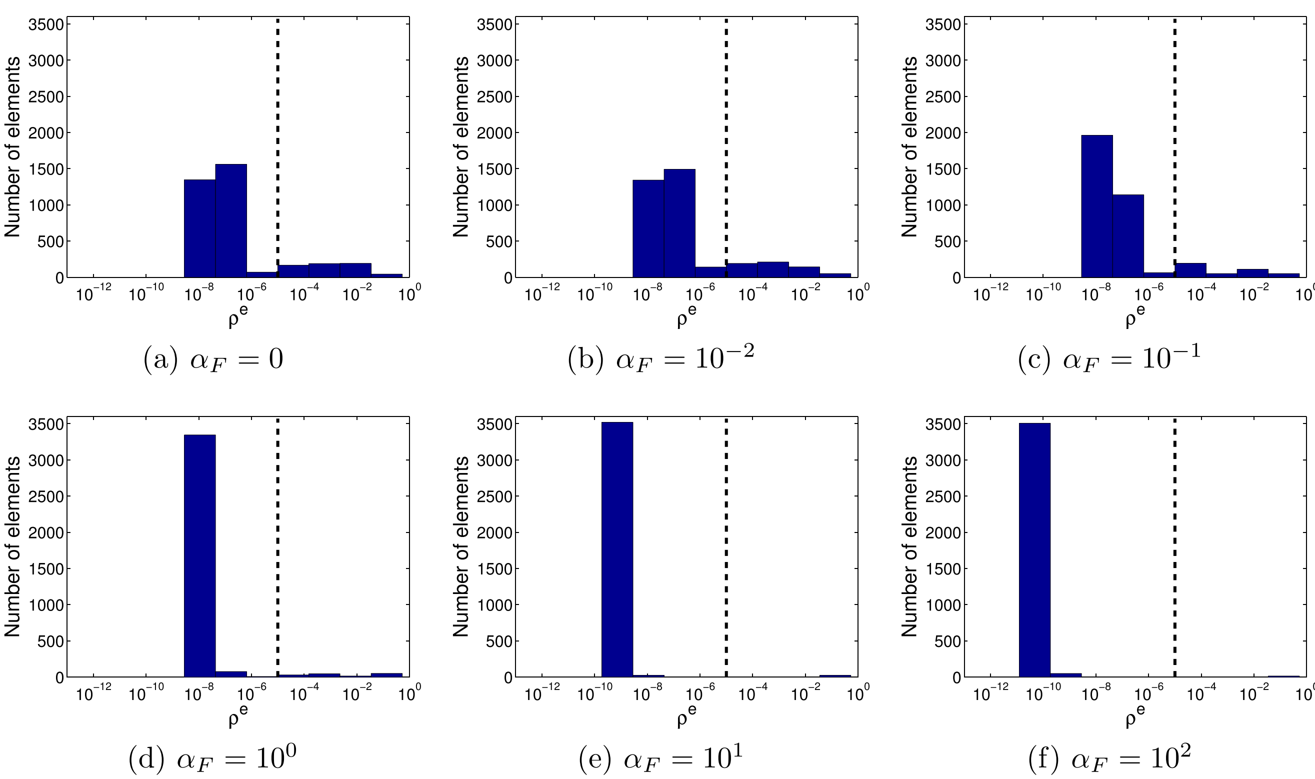

Fig. 4 Distribution of design variables for the simply supported truss domain shown in Fig. 1 after the first optimization convergence, i.e. before first element removal, for different values of α_F. *Dashed lines* in each figure indicate the threshold for removing elements at the end of each optimization iteration

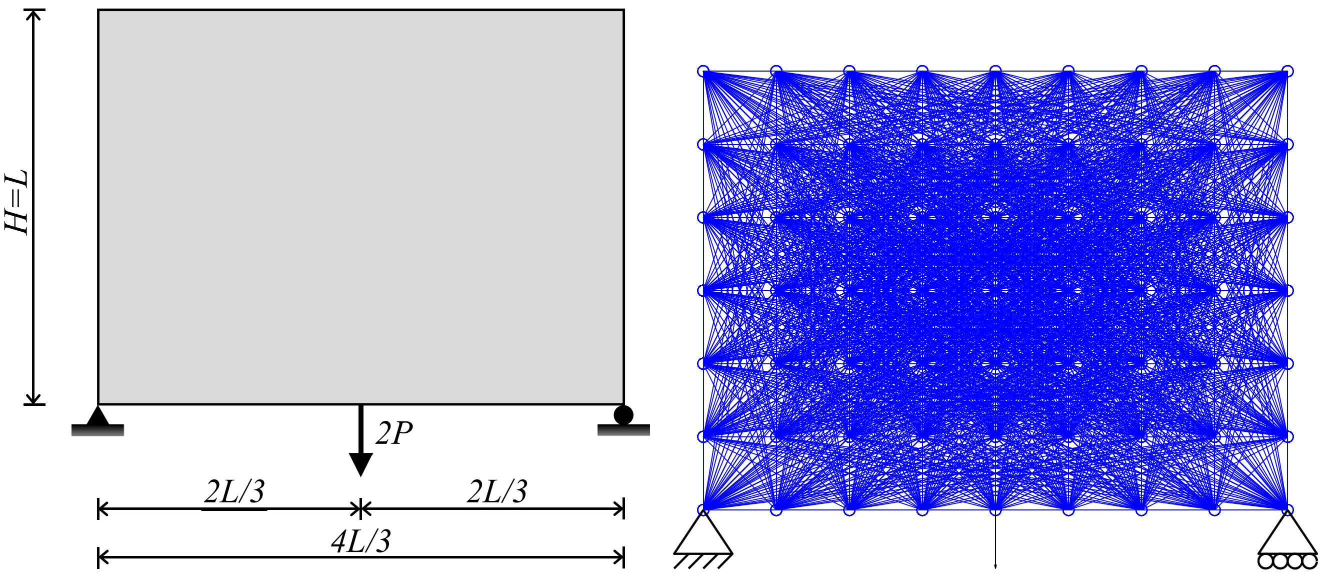

(a) Geometry and boundary conditions (b) Initial fully connected mesh

Fig. 5 **(a)** Geometry and boundary conditions for a simply supported truss domain with a point load on the bottom boundary; **(b)** initial fully connected mesh (*ground structure*) with 9 × 7 nodes and 1,953 truss elements

the domain between two supports is modeled. A 9 × 7-node mesh with 1,953 truss elements, shown in Fig. 5b, is used as the ground structure. As in the previous example, every pair of nodes in the mesh is connected by a truss element. The removal threshold for the elements is set to $\rho^e_{th} = 10^{-5}$, and the maximum allowable deflection at the midspan of the bottom boundary is $C^* = 240P/EL$.

The influence of fabrication cost on an optimized structure is demonstrated for α_W equal to $(15/L)^3$ and α_F equal to $\{0,\ 10^0,\ 10^1,\ 10^2,\ 10^3\}$, for a total of 5 independent optimization runs. Figure 6 displays optimized topologies for different values of α_F. For this discretization, the solution uses a relatively small number of elements when fabrication cost is not considered ($\alpha_F = 0$) (Fig. 6a). For small values of the fabrication cost ($\alpha_F = 10^1$), the optimal structure remains unchanged. When the unit fabrication cost is increased to $\alpha_F = 10^1$, the number of elements is reduced by 15 %, with further reductions observed for $\alpha_F = 10^2$ and $\alpha_F = 10^3$. As the $\alpha_F = 10^3$ structure is the simplest kinematically determinate topology, no further reduction in the number of elements is possible. The evolution of topology as a function of the unit fabrication cost is quantitatively displayed in Fig. 7. Values of fabrication cost and material cost (or weight) are normalized with the

Fig. 6 Optimized truss structures for the simply supported domain shown in Fig. 5 for different values of α_F

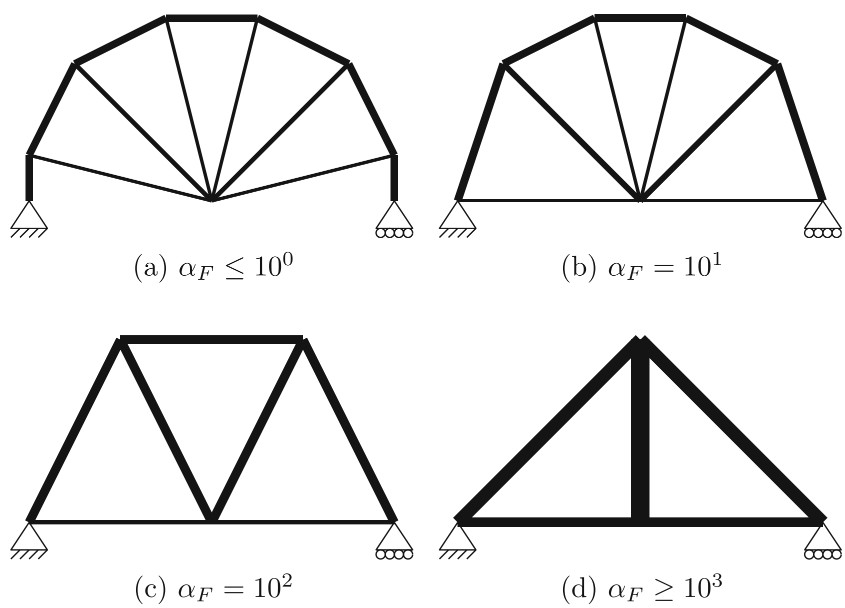

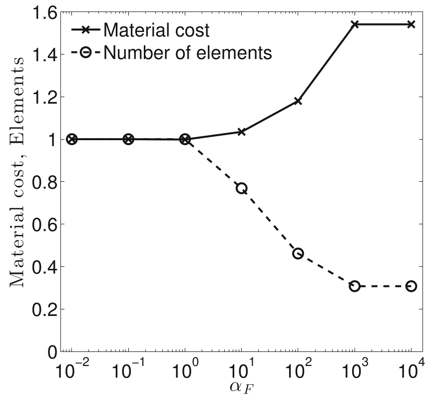

Fig. 7 Material cost and the number of elements in optimized structures for the domain shown in Fig. 5 for different values of α_F; All values are normalized with the corresponding value for the optimized structure shown in Fig. 6a with zero fabrication cost, i.e. $\alpha_F = 0$

corresponding value for the optimized $\alpha_F = 0$ structure (Fig. 6a). As expected, design complexity decreases and material cost increases with increasing fabrication cost parameter α_F in Fig. 7.

3.3 A periodic lattice subjected to effective axial and shear stiffness constraints

In this example we study a two-dimensional periodic lattice, defined by a unit cell, subjected to effective axial and shear stiffness constraints. This example is motivated by optimal design of sandwich panel cores, which demand a relatively high shear stiffness and a lower axial stiffness. We use the general optimization formulation stated in (7)–(10) with two total stiffness constraints: the effective Young's modulus in the horizontal direction and the effective shear modulus are constrained to 1 % and 10 % of the constituent material moduli, respectively. The effective properties of the unit cell are estimated by numerical homogenization (e.g., Guedes and Kikuchi (1990)), leading to an optimization problem that is often referred to as inverse homogenization (see e.g., Sigmund (1995) for additional discussion and detailed equations).

It is well known that unit cell topologies offering maximal stiffness may be non-unique, and this example displays multiple global minima with the same mass (material cost). As these minima are associated with different topologies, it makes the problem well suited for examining different fabrication cost scenarios, two of which are considered herein. The first scenario is uniform unit fabrication cost, where all elements have $\alpha_F^e = \alpha_F = 1$. In the second scenario, we express the element unit cost as a function of the element length. Specifically, elements whose length is half the length of the unit cell size incur the least fabrication cost, while the unit cost of longer and shorter elements increase by as much as a factor of twenty. The unit cost function is shown in Fig. 8a and given as $\alpha_F^e = 1 + 19|L^e/L - 0.5|/(\sqrt{2} - 0.5)$ where L is the length of the unit cell, L^e is the length of element e and $|\bullet|$ denotes the absolute value of $\bullet$. This scenario represents the situation where a specific length, here $L/2$, has minimum fabrication cost and any deviation from it results in extra fabrication costs. In both scenarios, it is assumed that $\alpha_W^e = \alpha_W = 1$.

Figure 8b depicts the ground structure of a fully connected lattice with 5×5 nodes, consisting of 300 truss elements connecting all the possible pairs of nodes in the unit cell. Periodic boundary conditions are applied using the same equation numbers for degrees of freedom opposing boundaries (e.g., Sigmund (1995)). Figure 9 illustrates the optimized unit cell for each of the fabrication cost scenarios, with each unit cell having the same material cost. When uniform fabrication cost is used, i.e. $\alpha_F^e = \alpha_F = 1$, a unit cell featuring a few long elements emerges. On the other hand, when unit fabrication cost is expressed as a non-uniform function of element length, as parameterized in Fig. 8a, with maximum unit fabrication cost of 11, the optimization algorithm designs a topology using several elements whose lengths are closer to $L/2$, the length corresponding to the cheapest unit cost. Despite requiring more elements, the total cost of this design is

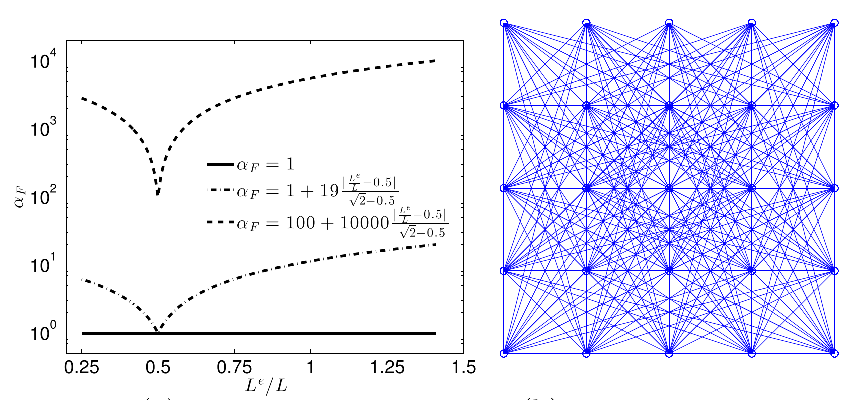

(a) Unit cost function (b) Initial fully connected mesh

Fig. 8 **(a)** Unit cost function used for different fabrication cost scenarios as a function of element length; **(b)** initial fully connected mesh (ground structure) with 5×5 nodes and 300 truss elements within the unit cell used for optimal design of a minimum-cost periodic lattice under effective axial and shear stiffness constraints. In this mesh, the length of elements varies from $L/4$ to $\sqrt{2}L$

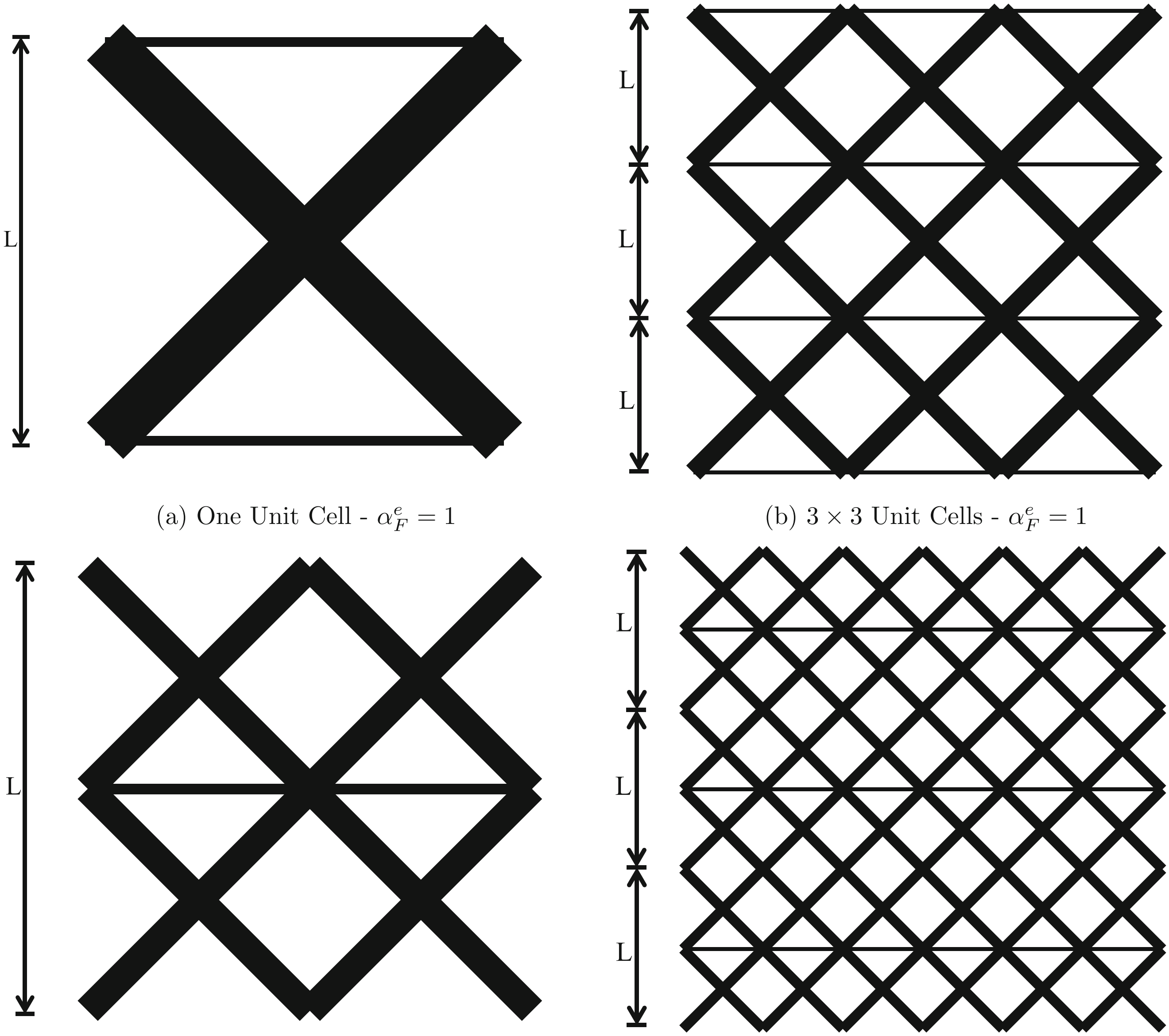

(a) One Unit Cell - $\alpha_F^e = 1$

(b) 3×3 Unit Cells - $\alpha_F^e = 1$

(c) One Unit Cell - $\alpha_F^e = 1 + 19\dfrac{|\frac{L^e}{L} - 0.5|}{\sqrt{2} - 0.5}$

(d) 3×3 Unit Cells - $\alpha_F^e = 1 + 19\dfrac{|\frac{L^e}{L} - 0.5|}{\sqrt{2} - 0.5}$

Fig. 9 Optimized periodic unit cells for the ground structure shown in Fig. 8b subjected to axial and shear stiffness constraints for two different fabrication cost scenarios plotted in Fig. 8a. First row shows the optimized solution for uniform unit cost of $\alpha_F^e = 1$ and the second row shows the optimized solution for nonuniform cost of $\alpha_F^e = 1 + 19|L^e/L - 0.5|/(\sqrt{2} - 0.5)$. Both optimized unit cells have the same minimal material cost

10 % lower than for the topology with fewer, longer elements, when evaluated using this nonuniform cost model. It should nevertheless be mentioned that each of these unit cells has minimum material cost, and thus could have been found by simply minimizing material cost using different initial guesses for the design variables. Considering fabrication cost, however, may lead to a unique minimum of the total cost problem, as illustrated here.

Interestingly, the topology significantly changes if we adjust the parameterization of the nonuniform fabrication cost scenario. For example, we further increase the expense of members whose length is different than $L/2$ by changing the unit cost structure to $\alpha_F^e = 100 + 10000|L^e/L - 0.5|/(\sqrt{2} - 0.5)$. This makes the fabrication cost for elements of length of $L/2$ equal to 100 units, and increases the maximum cost occurring for long diagonal elements to 10100 units. The resulting optimized solution is depicted in

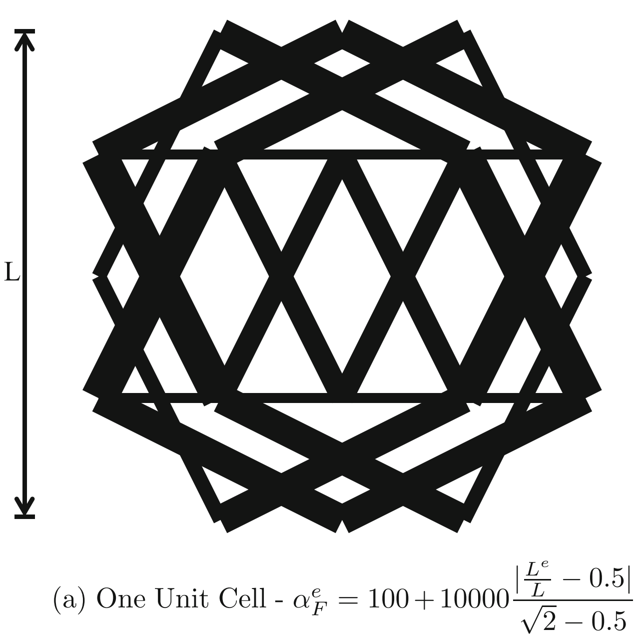

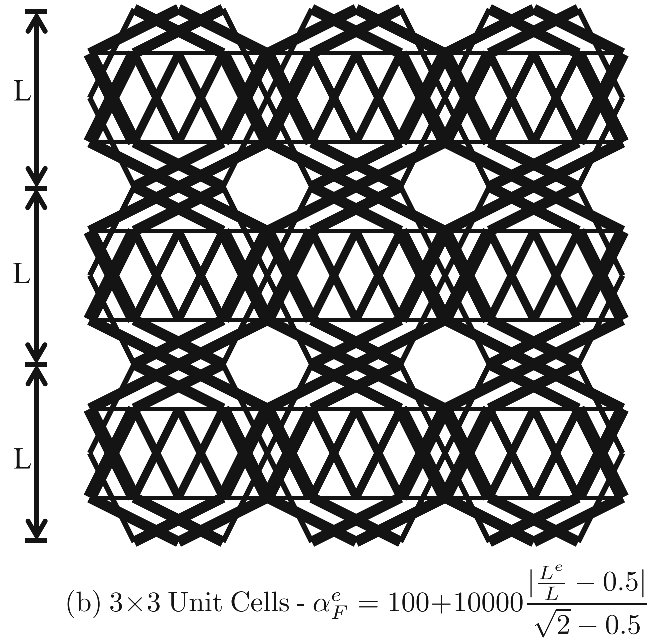

Fig. 10 Optimized unit cell for the ground structure shown in Fig. 8b for the fabrication cost with $\alpha_F^e = 100 + 10000|L^e/L - 0.5|/(\sqrt{2} - 0.5)$. This optimized unit cell consists of elements that are either $L/2$ or $\sqrt{1.25}L/2$ long

Fig. 10 and it is clearly seen that the algorithm has designed a topology that uses many more elements having length $L/2$ or $\sqrt{1.25}L/2$. This design change is done at the cost of material efficiency, as this design uses approximately 67 % more material to satisfy the stiffness constraints. The overall total cost, however, is significantly lower than the total cost of the previous unit cell designs when evaluated using this new fabrication cost model. Clearly the optimized lattice solution is dependent on the fabrication cost model, and the solution for the minimum material cost may not be optimal for the minimum total cost problem. On the other hand, for the uniform fabrication cost scenario, the optimized solution does not change by increasing the fabrication cost as it simultaneously possesses the least number of elements and the least material cost as opposed to previous structural examples.

3.4 Restricting the number of elements in a simply supported truss structure with a point load on the top boundary

As a final example, we look to design maximum stiffness (minimum deflection) structures using a limited number of members, as specified by the designer. This is achieved by solving the optimization problem stated by (15)–(18), with $\mathbf{L} = \mathbf{F}$, for the initial structure shown in Fig. 1. External geometry and boundary conditions are the same as in Section 3.1. The results found when varying the maximum allowable number of members between 3 and 100 are presented in Fig. 11. The maximum deflection and the mass of the structure, both normalized against the solution for $n_{el}^* = 3$, are plotted against the maximum allowable number of elements, n_{el}^*. Obviously, as the allowable number of elements is increased, the maximum deflection of the structure decreases (and hence the stiffness increases), while the mass of the structure increases. Note that weight is not minimized in this optimization problem, leading the optimizer to assign all members appearing in the final solution to have the maximum allowable cross-sectional area, A_{max}. Interestingly, stiffness and mass both increase nearly linearly with n_{el}^*; the implication is that all the designs in Fig. 11 have nearly identical structural efficiency (i.e., stiffness/mass). In this

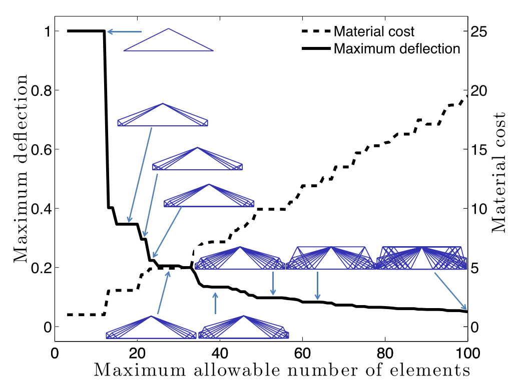

Fig. 11 Amount of material and maximum deflection of optimized structures for minimizing maximum deflection for the initial structure shown in Fig. 1 for different maximum number of elements, i.e. n_{el}^*. All values are normalized with the corresponding value for the optimized structure with three elements, i.e. $n_{el}^* = 3$

case, the conclusion is that increasing the complexity of the topology presents insignificant benefit in terms of specific stiffness (albeit, there might be advantages from the perspective of strength and/or robustness).

Another interesting conclusion that emerges from the results plotted in Fig. 11 is that intervals of n^*_{el} exist within which the solution does not change (for example, $n^*_{el} \in [3\ 12]$, $n^*_{el} \in [15\ 20]$, and $n^*_{el} \in [25\ 30]$). This happens because adding very few extra elements to these optimized structures is not sufficient to develop new load carrying paths, and thus the optimizer has no incentive to add elements in these cases. Notice that in some instances, adding members actually leads to a decrease in material cost (mass), even though these members achieve A_{max}. This is because elements have different lengths and there is no constraint imposed on the total material cost in the structure.

Finally, it is worth emphasizing the importance of using the nonlinear (regularized) Heaviside step function in (17) to approximate the number of elements used in the design. The output of this function for a small value, e.g. $\rho^e = 0.01$, and a large value, e.g. $\rho^e = 1$, would be approximately one in both cases as long as a sufficiently large value for parameter β is employed (e.g., $\beta = 1000$ is used herein). This is critical if members with these cross-sectional areas are to each count as one member used in the design; the same feature could not be achieved with (for example) a simple summation on all ρ^e.

4 Conclusions

This article proposes a method to incorporate fabrication cost in topology optimization of discrete structures, i.e., trusses and/or periodic lattices. The fabrication cost is modeled by assigning each element in the mesh a unit cost. The idea is that any designed element requires installation and two connections, and that these are treated as discrete, fixed per element costs. A regularized Heaviside step function is adopted to render the objective function smooth and differentiable. The proposed algorithm is demonstrated on classic examples from structural engineering and on the design of a unit cell of a periodic material; in both cases, the evolutions of optimal topology, mass (or material cost) and fabrication cost of the structure are tracked as a function of the fabrication unit cost (and hence the relative 'cost of complexity'). As expected, increasing the fabrication unit cost results in optimized structures with fewer elements and simpler designs. Typically, this comes at the expense of structural efficiency, and thus induces an increase in mass (or material cost) in order to satisfy structural constraints.

Interestingly, if sufficiently large fabrication unit costs are chosen, the proposed objective function significantly accelerates convergence and reduces computational time for mass minimization problems under stiffness constraints. This is due to the fact that the optimizer pushes low magnitude design variables (i.e., small cross-sectional areas) to zero as such elements are inefficient in terms of fabrication cost. This also makes the process of identifying elements to be removed very objective, thereby reducing solution dependence on the arbitrary threshold variable typically used to identify such elements. It may therefore serve as a useful and physically meaningful penalization function to promote elimination of inefficient elements in general truss and frame topology optimization.

It is worth noting that the methodology requires quantification of parameters α^e_W and α^e_F, the unit material cost and unit fabrication cost, respectively. Ideally, these unit costs would be input by the designer based on local market rates for materials and labor (or automated fabrication processes), and the algorithm would output the lowest cost structure. While materials costs may be straightforward to estimate, fabrication costs are significantly more complicated, typically requiring input from local construction experts. We have also limited our discussion of fabrication costs to member placement and connections. These functions can surely be made more complicated, such as making placement and connection costs a function of member mass and cross-section dimensions.

Regardless, even for situations where the fabrication unit cost (or the allowable number of elements) is unknown a priori, the presented approach can provide the designer with a quick assessment of the complexity/cost benefits in topology optimization. Finally, it is anticipated that this algorithm would work for more complex problems, where more elaborate mechanical objectives and constraints are formulated. For example, it would also be interesting to combine the approach with recent work focusing on improving the robustness of truss structures under fabrication flaws. Robustness may often be improved through diversification of the load path, resulting in increased complexity of the optimized topology (Asadpoure et al. 2011; Jalalpour et al. 2011). Introducing a cost to this complexity, as done here, could lead to more realistic optimized structures.

Acknowledgments This work was financially supported by the Office of Naval Research under Grant No. N00014-11-1-0884 (program manager: D. Shifler). This support is gratefully acknowledged. The authors are also thankful to Krister Svanberg for providing the MMA optimizer subroutine.

References

Achtziger W, Stolpe M (2006) Truss topology optimization with discrete design variables—Guaranteed global optimality and benchmark examples. Struct Multidiscip Optim 34(1):1–20. doi:10.1007/s00158-006-0074-2

Achtziger W, Stolpe M (2007a) Global optimization of truss topology with discrete bar areas—Part I: theory of relaxed problems. Comput Optim Appl 40(2):247–280. doi:10.1007/s10589-007-9138-5

Achtziger W, Stolpe M (2007b) Global optimization of truss topology with discrete bar areas—Part II: Implementation and numerical results. Comput Optim Appl 44(2):315–341. doi:10.1007/s10589-007-9152-7

Ambrosio L, Buttazzo G (1993) An optimal design problem with perimeter penalization. Calc Var 1(1):55–69. doi:10.1007/BF02163264

Amir O, Sigmund O (2013) Reinforcement layout design for concrete structures based on continuum damage and truss topology optimization. Struct Multidiscip Optim 47(2):157–174. doi:10.1007/s00158-012-0817-1

Asadpoure A, Tootkaboni MP, Guest JK (2011) Robust topology optimization of structures with uncertainties in stiffness—Application to truss structures. Comput Struct 89(11–12):1131–1141. doi:10.1016/j.compstruc.2010.11.004

Ben-Tal A, Bendsøe MP (1993) A new method for optimal truss topology design. SIAM J Optim 2:322–358. doi:10.1137/0803015

Bendsøe MP (1989) Optimal shape design as a material distribution problem. Struct Optim 1(4):193–202. doi:10.1007/BF01650949

Bendsøe MP, Ben-Tal A, Zowe J (1994) Optimization methods for truss geometry and topology design. Structural Optimization 7(3):141–159. doi:10.1007/BF01742459

Bendsøe MP, Sigmund O (2003) Topology Optimization: Theory, Methods and Applications. Springer

Dorn William S, Gomory Ralph E, Greenberg Herbert J (1964) Automatic design of optimal structures. Journal de Mecanique 3(1):25–52

Groenwold AA, Stander N, Snyman JA (1996) A pseudo-discrete rounding method for structural optimization. Struct Optim 11(3–4):218–227. doi:10.1007/BF01197037

Guedes JM, Kikuchi N (1990) Preprocessing and postprocessing for materials based on the homogenization method with adaptive finite element methods. Comput Methods Appl Mech Eng 83(2):143–198. doi:10.1016/0045-7825(90)90148-F

Guest JK (2009) Topology optimization with multiple phase projection. Comput Methods Appl Mech Eng 199(1–4):123–135. doi:10.1016/j.cma.2009.09.023

Guest JK, Asadpoure A, Ha S-H (2011) Eliminating beta-continuation from Heaviside projection and density filter algorithms. Struct Multidiscip Optim. doi:10.1007/s00158-011-0676-1

Guest JK, Prévost JH, Belytschko TB (2004) Achieving minimum length scale in topology optimization using nodal design variables and projection functions. Int J Numer Methods Eng 61(2):238–254. doi:10.1002/nme.1064

Haber RB, Jog CS, Bendsøe MP (1996) A new approach to variable-topology shape design using a constraint on perimeter. Struct Optim 11(1–2):1–12. doi:10.1007/BF01279647

Jalalpour M, Igusa T, Guest JK (2011) Optimal design of trusses with geometric imperfections: Accounting for global instability. Int J Solids Struct 48(21):3011–3019. doi:10.1016/j.ijsolstr.2011.06.020

Jog CS, Haber RB, Bendsøe MP (1994) Topology design with optimized, self-adaptive materials. Int J Numer Methods Eng 37(8):1323–1350. doi:10.1002/nme.1620370805

Parkes EW (1975) Joints in optimum frameworks. Int J Solids Struct 11(9):1017–1022. doi:10.1016/0020-7683(75)90044-X

Poulsen TA (2003) A new scheme for imposing a minimum length scale in topology optimization. Int J Numer Methods Eng 57(6):741–760. doi:10.1002/nme.694

Rozvany GIN (1996) Difficulties in truss topology optimization with stress, local buckling and system stability constraints. Struct Optim 11(3–4):213–217. doi:10.1007/BF01197036

Rozvany GIN (2011) On symmetry and non-uniqueness in exact topology optimization. Struct Multidiscip Optim 43(3):297–317. doi:10.1007/s00158-010-0564-0

Sigmund O (1995) Tailoring materials with prescribed elastic properties. Mech Mater 20(4):351–368. doi: 10.1016/0167-6636(94)00069-7

Sigmund O (2007) Morphology-based black and white filters for topology optimization. Struct Multidiscip Optim 33(4–5):401–424. doi:10.1007/s00158-006-0087-x

Stolpe M (2004) Global optimization of minimum weight truss topology problems with stress, displacement, and local buckling constraints using branch-and-bound. Int J Numer Methods Eng 61(8):1270–1309. doi:10.1002/nme.1112

Svanberg K (1987) The method of moving asymptotesa new method for structural optimization. Int J Numer Methods Eng 24(2): 359–373. doi:10.1002/nme.1620240207

Svanberg K (1995) A globally convergent version of MMA without linesearch. In: Olhoff N, Rozvany GIN (eds) Proceedings of the First World Congress of Structural and Multidisciplinary Optimization. Pergamon Press, Elmsford, pp 6–16

Zhou M, Rozvany GIN (1991) The COC algorithm, Part II: Topological, geometrical and generalized shape optimization. Comput Methods Appl Mech Eng 89(1–3):309–336. doi:10.1016/0045-7825(91)90046-9

Mu Z, Yang Y, Gaynor AT, Guest JK (2014) Considering Constructability in Structural Topology Optimization. In: Structures Congress 2014. American Society of Civil Engineers, Reston, pp 2754–2764. doi:10.1061/9780784413357.241